



Published in final edited form as:

*Ultrasound Med Biol.* 2020 January ; 46(1): 149–155. doi:10.1016/j.ultrasmedbio.2019.08.020.

## Quantitative ultrasound detects smooth muscle activity at the cervical internal os *in vitro*

Andrew P. Santoso<sup>a</sup>, Joy Y. Vink<sup>b</sup>, George Gallos<sup>c</sup>, Helen Feltovich<sup>a,d</sup>, Timothy J. Hall<sup>a,\*</sup>

<sup>a</sup>Department of Medical Physics, University of Wisconsin-Madison, Madison, WI

<sup>b</sup>Department of Obstetrics & Gynecology, Columbia University Medical Center, New York, NY

<sup>c</sup>Department of Anesthesiology, Columbia University Medical Center, New York, NY

<sup>d</sup>Maternal Fetal Medicine, Intermountain Healthcare, Provo, UT

### Abstract

The cervix has two biomechanical functions: to remain closed while the fetus develops throughout pregnancy, then open for delivery of the fetus at full-term. This dual function is principally attributed to collagen within the extracellular matrix (ECM). However, recent evidence suggests that other ECM, and non-ECM, components play a role as well. One component is smooth muscle cells (SMC) arranged circumferentially near the internal os. In this study, we investigate correlations between cervical SMC force generation and the effective scatterer diameter (ESD), a quantitative ultrasound parameter directly related to the acoustic impedance distribution, and therefore a potential biomarker of muscle contractility. Using whole cervical slices (N=5), we determined significant positive correlations (quantified with Pearson's  $r$ ) between muscle force generation and ESD immediately after administration of oxytocin (median  $r=0.90$ ). In summary, the ESD may prove a useful biomarker for studying structure and function of cervical smooth muscle *in vivo*.

### Keywords

Cervical assessment; Cervical smooth muscle; Effective scatterer diameter; Internal os architecture; Quantitative ultrasound

### Introduction

Birth is a universal occurrence, yet surprisingly little is understood about the tissue remodeling processes that facilitate mammalian parturition. Pregnancy tissues must undergo dramatic and precisely timed change during pregnancy; the uterus must first remain quiet and then contract, the membranes strong and then rupture, and the cervix closed and stiff

\*Corresponding Author: Timothy J. Hall, Department of Medical Physics, University of Wisconsin-Madison, 1111 Highland Avenue, Rm 1005, Madison, WI 53705 USA; tjhall@wisc.edu; Phone, 608-265-9459.

**Publisher's Disclaimer:** This is a PDF file of an unedited manuscript that has been accepted for publication. As a service to our customers we are providing this early version of the manuscript. The manuscript will undergo copyediting, typesetting, and review of the resulting proof before it is published in its final citable form. Please note that during the production process errors may be discovered which could affect the content, and all legal disclaimers that apply to the journal pertain.

and then soften and open. To optimize outcomes for mothers and newborns, this must all happen at the right time for delivery to occur at term (37 to 40 weeks of gestation), instead of too early or too late. The cervix is a logical target for investigation of parturition for two reasons: it is the final obvious gateway to delivery since it must open for the fetus to deliver vaginally, and it is easily accessible. Today's dogma is that changes in extracellular matrix (ECM) collagen are primarily responsible for the remarkable biomechanical plasticity of the cervix, with only minor contributions from other ECM, or non-ECM, components (Danforth, 1947; Vink and Feltovich, 2016). One such component, smooth muscle cells (SMC), is considered sparse, randomly disseminated, and nonfunctional (Hughesdon, 1952; Danforth, 1983) and for this reason SMC have been largely overlooked in study of cervical structure and function.

Recent findings, however, suggest a more active role for cervical SMC. Vink et al. (2016) found a gradient of SMC along the cervix using immunohistochemistry techniques, with most SMC arranged circumferentially near the area of the internal cervical os, where the cervix opens into the uterus. A magnetic resonance imaging study by Nott et al. corroborated this finding; they identified a circumferential "occlusive structures" in the area of the internal os (Nott et al., 2017). These studies suggest that SMC are not sparse or randomly disseminated. Further, they appear to be functional; when whole transverse slices of cervical tissue were exposed to oxytocin (a contractile agent) in functional organ baths, the area of the internal os demonstrated a twofold greater integrated force than the external os (the opening of the cervix into the vagina) (Vink et al., 2016). Taken together, these findings suggest that cervical SMC may function as a sphincter at the internal os.

These findings are interesting because this area of the internal os, where the uterus, membranes, and cervix meet, is where cervical change during pregnancy initiates. When transvaginal ultrasound became widely used in the 1990s, a phenomenon called "funneling" in this area was noted; it described the process of the cervix shortening and dilating, as the membranes protrude into the cervical canal, in preparation for delivery (Ziliani et al., 1995). It is therefore not unexpected that a sphincter might be found at this intersection. Although the IHC, imaging and functional studies described above are recent, the concept of a functional cervical sphincter is more than a century old; in 1872 Lott described a "sphincter isthmii interni based on cadaver studies, and in 1924 Oertel suggested that it was functional, as reported in Youssef (1958). Studies from the 1930s through 1990s reported that the cervix and uterus of pregnant and nonpregnant women contract independently in response to hormones or oxytocin *in vivo* and that cervical tissue contracts when exposed to adrenoreceptor agonists or oxytocin in organ baths (Karlson, 1949; Schild et al., 1951; Youssef, 1958; Mackenzie, 1976; Bryman et al., 1984; Olah, 1993).

Until recently, a noninvasive means of evaluating potential SMC function in the cervix did not exist but fortunately, quantitative ultrasound (QUS) approaches to assess both tissue structure and function are emerging. Parameters derived from the acoustic backscatter coefficient (BSC) have been shown to be directly related to the underlying specific acoustic impedance (the product of mass density and sound speed) (Insana et al., 1990). Such parameters have been used to identify geometric changes, for example, due to muscle contraction/relaxation throughout the cardiac cycle in canine myocardium (Madaras et al.,

1983; Wear et al., 1989). The BSC frequency-dependence can be parameterized via the effective scatterer diameter (ESD), which estimates effective sizes of structures interacting with ultrasound waves along the direction of propagation (Insana et al., 1990). Therefore, it seems reasonable that if the putative sphincter at the internal os is functional, i.e. contracts, the ESD could detect that activity and serve as a biomarker of cervical muscle activity. If so, further development of the approach proposed here could lead to a non-invasive, ultrasound-based method to observe cervical function *in vivo*, which could in turn lead to an improved understanding of parturition and novel therapeutic approaches to dysfunctional parturition such as pre-term or post-dates birth.

The goal of this study was to take the first step along that investigative pathway, specifically, to determine whether the ESD correlates with force generation at the internal os of the cervix *in vitro*.

## Materials and Methods

### Tissue acquisition

Cervical specimens were obtained from nonpregnant, premenopausal women undergoing hysterectomy for benign indications under an IRB-approved protocol (#IRB-AAAI0337) at Columbia University Medical Center, New York, NY, USA. Written informed consent was obtained from all women. Whole transverse slices of 6.0 to 10.0 mm thickness (N=5) were obtained from the region of the internal os, and immediately placed in ice-cold SmBM2 media with recommended additives (Lonza, Walkersville, MD, USA).

### Data acquisition

Each slice of cervical tissue was suspended via sutures in a 300 mL water-jacketed organ bath (Radnoti Glass Technology, Monrovia, CA) with one end of the tissue attached to the bottom of the bath and the other end attached to a Grass FT03 force transducer (Grass-Telefactor, West Warwick, RI, USA; see Figure 1). The baths were filled with a modified Krebs-Henseleit buffer (Quan et al., 2003; Vink et al., 2016) continuously bubbled with 95% oxygen/5% carbon dioxide, and kept at 37°C. Specimens were allowed to equilibrate to isometric tension for 1 hour. Muscle force generation data were digitized from the force transducer with BIOPAC hardware (MP150, 16-bit A/D resolution) and using AcqKnowledge software (BIOPAC Systems Inc, Goleta, CA, USA) at a sampling rate of 1 Hz.

Radiofrequency (RF) echo data were collected with a Siemens Acuson S3000 system (Siemens Healthcare, Ultrasound Business Unit, Mountain View, CA, USA) and a 14L5SP linear array transducer operated at a center frequency of 10 MHz using the Axius Direct ultrasound research interface (Brunke et al., 2007). A transducer cover filled with coupling gel was used as a protective barrier between the linear array and the organ bath solution. Sound absorbing rubber was placed in the organ bath to minimize reverberation signal from the glass. The transducer was fixed to a 5-axis mechanical stage with the imaging plane roughly parallel to the endocervical canal. RF echo signal frames were acquired before and after administration of 1.0  $\mu$ M of oxytocin (Sigma-Aldrich, St. Louis, MO, USA) (Bryman

et al., 1990) at a sampling rate of 1 RF echo signal frame every 2 seconds from 5 minutes before, and up to 5 hours after, oxytocin administration. The experimental setup and a representative B-mode image are shown in Figure 1.

Immediately after RF data acquisition for each sample, 20 independent planes of reference phantom data were collected with the same system settings and transducer. This reference phantom was composed of water-based gel (4.5 g/L; BD Bacto Dehydrated Agar, Becton, Dickinson and Company, Franklin Lakes, NJ, USA) containing graphite powder (50 g/L; Superior Graphite, Chicago, IL, USA) and glass beads (4 g/L, 3000E beads; ~5–20  $\mu\text{m}$ , Potters Industries, Malvern, PA, USA). Acoustic properties of the reference phantom were independently measured, as reported by Hall et al. (1996). The average sound speed measured over the bandwidth was  $1567 \text{ m}\cdot\text{s}^{-1}$ . The attenuation coefficient fit to a power law yielded attenuation of  $0.5 \text{ dB}\cdot\text{cm}^{-1}\cdot\text{MHz}^{-1.1}$ .

### Data processing

Specimen BSCs for every time point were estimated using the Reference Phantom Method (Yao et al., 1990). Assuming scattering is sufficiently weak to ignore multiple scattering (Born approximation) and the distance to the region of interest (ROI) is larger than the maximum dimension of the two-dimensional transducer aperture, the power spectrum  $S$  of the backscattered RF echo signals is given by:

$$S(f, z) = G(f)D(f, z)A(f, z)BSC(f) \quad (1)$$

where  $f$  is the temporal frequency and  $z$  is the depth to the center of the ROI.  $G(f)$  represents the combined transducer effects from transmitting and receiving the RF signal,  $D(f)$  represents diffraction effects, and  $A(f,z)$  is the total attenuation from intervening media between the transducer and the center of the ROI.

Data processing was performed off-line using MATLAB (MathWorks, Natick, MA, USA). Using the methods described by Thijssen (2003), axial and lateral RF echo signal correlation lengths were estimated to be  $191 \mu\text{m}$  and  $281 \mu\text{m}$ , respectively, in the reference phantom. Samples were manually segmented (in ImageJ; open source software available at [imagej.net](http://imagej.net)) from the buffer background and stationary  $5\times 5 \text{ mm}^2$  ROIs (see Figure 1) were used to estimate power spectra over the duration of data acquisition. This ROI size was determined following the recommendations of Rosado-Mendez et al. (2013) to obtain optimal backscatter parameter estimates. The center of mass (CoM) of the B-mode image area showing cervix tissue was estimated and deviations in the location of the CoM were estimated to ensure use of a stationary ROI was appropriate (Schneider et al., 2012). Sample power spectra were divided by the reference phantom power spectra for ROIs at the same spatial location to remove system effects. Power spectra were estimated using a multitaper method (Thomson, 1982) with 5 tapers. Attenuation compensation in the samples was accomplished by using published median attenuation coefficient values from our previous study of the *ex vivo* human cervix (see Guerrero et al. (2018)).

## BSC parameterization: Frequency dependence of backscatter

We studied the effective scatterer diameter (ESD), a BSC parameter that quantifies the spatial correlation length of the acoustic impedance distribution (Insana et al., 1990). Parameterization was performed over a 4–9 MHz bandwidth and done for every time point, allowing for a direct comparison between force generation and backscatter parameter time series.

It has been extensively shown that Gaussian correlation functions are well-suited to describe scattering sources with continuously varying fluctuations in acoustic impedance or in the presence of narrow diameter distributions of discrete scatterers (Gerig et al., 2003; Nordberg and Hall, 2015; Zagzebski et al., 2016). Acoustic form factors, functions proportional to the Fourier transform of the correlation function, may be estimated from BSCs directly (Insana and Hall, 1990), whereby deviation from  $r^4$  Rayleigh scattering can be, in special cases (e.g., Bowman's capsule in the renal cortex), attributed to the finite size of the scatterer. ESDs were estimated using a Gaussian form factor model and a modified least squares estimator for the cervix specimens providing information regarding subresolution scattering sources (Gerig et al., 2003).

## Time series analysis

Comparison between the force generation and ESD time series was accomplished via calculation of the Pearson correlation coefficient  $r$ . This was done using non-overlapping moving time windows in 5 minute increments over the first 30 minutes after oxytocin administration (i.e., six temporally independent time windows). Prior to calculation of  $r$ , force generation data were downsampled to match ESD sampling and a 30-second moving average filter was applied to both parameters to reduce high frequency estimate variance.

## Results

B-mode videos of a cervix specimen before and after administration of oxytocin are provided in Videos 1 and 2, respectively. Figure 2 provides an example of a CoM deviation curve. While it should be noted that bulk motion was visually appreciable in Video 2, CoM deviations in all specimens were smaller than 1.0 mm. This provides confidence that changes in ESD are due to changes in cervical microstructure rather than bulk motion.

Representative time series curves are provided in Figure 3, highlighting differences before and after applying the moving average filter. Results of the Pearson correlation between force generation and ESD before and after applying the moving average filter are provided in Figure 4. For the filtered data, the median  $r$  was positive and maximal in the early time window ( $r=0.90$ , 0–5 minutes), primarily decreasing as time increased, while maintaining positive median correlations throughout the duration of measurements, and reaching a stable value ( $r=0.30$ ) at the 20–25 minute time window.

## Discussion

Understanding the function of biological tissues is facilitated by biomarkers that can detect and quantify microstructural changes within that tissue. Currently, to our knowledge, there

are no biomarkers that can assess cervical tissue function *in vivo*; medical imaging tools such as optical microscopy and magnetic resonance imaging have been used to describe *in vitro* and *ex vivo* cervical microstructure, but they cannot assess *in vivo* function (Vink et al., 2016; Nott et al., 2017). The purpose of this study was to explore whether a QUS parameter, the ESD, could detect force generation (presumably due to muscle fiber contraction/relaxation cycles) in SMC near the internal os of the cervix *in vitro*. In brief, we found that the ESD strongly correlates with force generation in excised cervical tissue, particularly within the first five-minute time window after administration of oxytocin.

The ESD parameter is a direct measure of the acoustic impedance distribution, based on the underlying theory that an acoustic impedance mismatch between intracellular and extracellular matrix components leads to ultrasonic scattering (Wickline et al., 1985). As such, it can provide information about muscle contraction and relaxation. Indeed, changes in scattering have been shown to correlate with contraction/relaxation cycles in canine myocardium (Madaras et al., 1983; Wear et al., 1989). Similarly, in our study we found that variability in the ESD correlated strongly with force generation in excised cervical tissue, particularly at the internal os where a ring of SMC has been identified. The purpose of this study was simply to determine whether ESD is measurable in cervical tissue, but, excitingly, it is reasonable to assume that the cyclic changes in ESD are due to muscle contraction/relaxation cycles. Confirming this will be the subject of future study.

The primary limitation of this study is that the tissue was obtained from nonpregnant women. We chose this approach because obtaining tissue from pregnant women is impractical and we were not overly concerned about using tissue from nonpregnant women because Bryman et al. (1990) demonstrated equal sensitivity to oxytocin in cervical tissue from women who were pregnant or not pregnant. Another potential limitation of this approach is the relatively large range in correlations between muscle force generation and ESD across specimens. This is likely explained by biological variability, however, which will be thoroughly investigated in future studies.

Interestingly, we observed asynchrony at two time points: immediately after oxytocin administration and 15 minutes after the experiment started. Specifically, there was a strong correlation prior to oxytocin administration, as well as at the 5–10 minute post-oxytocin time window, after which force generation and ESD correlations were reduced, reaching a stable  $r$  by the 20–25 minute time window. Further study is necessary to confirm our suspicions, but we can reasonably assume that these observations are explained by our experimental setup. Specifically, for valid backscatter measurements, the ESD must be estimated away from tissue boundaries (i.e. in the center rather than the periphery of the tissue), and the tissue thickness must be at least 5 mm (as opposed to 3 mm used in our initial study of force generation in cervical tissue) (Liu et al., 2010; Vink et al., 2016). Because the experiment relied upon diffusion for oxytocin delivery, it is logical that it would take more time for the drug to reach the center of the tissue than its periphery, and therefore the latter would exhibit contractile force before the center, creating dyssynchrony. Regarding the irregularity of both curves after the 10–15 minute time window, it is reasonable to assume that the effects of oxytocin diminish over time, and/or that the muscle reached its maximum ability to contract and started to fail. This speculation is interesting, and will be

explored in future studies of both *ex vivo* tissue, and *in vivo*. However, the simple objective of this study was to evaluate the potential of ESD as a biomarker of muscle activity in the cervix, and the strong correlation between ESD and force generation suggest that the parameter certainly has potential.

## Conclusions

This study demonstrated that the ESD, a quantitative ultrasound parameter, correlates with cervical SMC force contractility in tissue in organ baths. Future studies will address whether SMC contractility can be identified in pregnant women. If so, we will explore the relevance of the ESD biomarker to specific applications, for example, whether there is a “normal” level of SMC force contractility, and whether abnormal contractility is associated with parturition complications such as pre-term or post-dates labor.

## Supplementary Material

Refer to Web version on PubMed Central for supplementary material.

## Acknowledgements

We are grateful for the technical support and equipment loan from Siemens Ultrasound. Additionally, we wish to acknowledge the women who kindly gave consent to participate in this research at Columbia University Medical Center. Research reported in this publication was supported by National Institutes of Health Grants T32CA009206 from the National Cancer Institute and R21HD061896, R21HD063031, R01HD072077, R01HD082251, and K08HD088758 from the Eunice Kennedy Shriver National Institute of Child Health and Human Development. The content is solely the responsibility of the authors and does not necessarily represent the official views of the National Institutes of Health.

## References

- Brunke SS, Insana MF, Dahl JJ, Hansen C, Ashfaq M, Ermert H. An ultrasound research interface for a clinical system. *IEEE Trans Ultrason Ferroelectr Freq Control*, 2007;54:198–210. [PubMed: 17225815]
- Bryman I, Lindblom B, Norstrom A, Sahni S. Adrenoceptor mechanisms in the regulation of contractile activity in the human cervix. *Obstet Gynecol*, 1984;64:363–367. [PubMed: 6146956]
- Bryman I, Norstrom A, Lindblom B. Influence of neurohypophyseal hormones on human cervical smooth muscle contractility in vitro. *Obstet Gynecol*, 1990;75:240–243. [PubMed: 2300351]
- Danforth DN. The fibrous nature of the human cervix, and its relation to the isthmic segment in gravid and nongravid uteri. *Am J Obstet Gynecol*, 1947;53:541–560.
- Danforth DN. The morphology of the human cervix. *Clin Obstet Gynecol*, 1983;26:7–13. [PubMed: 6839572]
- Gerig A, Zagzebski J, Varghese T. Statistics of ultrasonic scatterer size estimation with a reference phantom. *J Acoust Soc Am*, 2003;113:3430–3437. [PubMed: 12822813]
- Guerrero QW, Feltovich H, Rosado-Mendez IM, Carlson LC, Li G, Hall TJ. Anisotropy and Spatial Heterogeneity in Quantitative Ultrasound Parameters: Relevance to the Study of the Human Cervix. *Ultrasound Med Biol*, 2018;44:1493–1503. [PubMed: 29661482]
- Hall TJ, Insana MF, Harrison LA, Cox GG. Ultrasonic measurement of glomerular diameters in normal adult humans. *Ultrasound Med Biol*, 1996;22:987–997. [PubMed: 9004422]
- Hughesdon PE. The fibromuscular structure of the cervix and its changes during pregnancy and labour. *BJOG*, 1952;59:763–776.
- Insana MF, Hall TJ. Parametric ultrasound imaging from backscatter coefficient measurements: Image formation and interpretation. *Ultrason Imaging*, 1990;12:245–267. [PubMed: 1701584]

- Insana MF, Wagner RF, Brown DG, Hall TJ. Describing small-scale structure in random media using pulse-echo ultrasound. *J Acoust Soc Am*, 1990;87:179–192. [PubMed: 2299033]
- Karlson S On the motility of the uterus during labour and the influence of the motility pattern on the duration of labour. *Acta Obstet Gynecol Scand*, 1949;28:209–250. [PubMed: 18141659]
- Liu W, Zagzebski JA, Liu W. Trade-Offs in Data Acquisition and Processing Parameters for Backscatter and Scatterer Size Estimations. *IEEE Trans Ultrason Ferroelectr Freq Control*, 2010;57:340–352. [PubMed: 20178900]
- Mackenzie I The effects of oxytocics on the human cervix during midtrimester pregnancy. *BJOG*, 1976;83:780–785.
- Madaras EI, Barzilai B, Perez JE, Sobel BE, Miller JG. Changes in myocardial backscatter throughout the cardiac cycle. *Ultrason Imaging*, 1983;5:229–239. [PubMed: 6685368]
- Nordberg EP, Hall TJ. Effective Scatterer Diameter Estimates for Broad Scatterer Size Distributions. *Ultrason Imaging*, 2015;37:3–21. [PubMed: 24831300]
- Nott J, Pervolaraki E, Benson A, Bonney E, Pickering J, Wilkinson N, Simpson N. Diffusion tensor imaging determines three-dimensional architecture of human cervix: a cross-sectional study. *BJOG: An International Journal of Obstetrics & Gynaecology*, 2017;125:818–818.
- Olah KS. Cervical contractions: the response of the cervix to oxytocic stimulation in the latent phase of labour. *BJOG*, 1993;100:635–640.
- Quan A, Leung SWS, Lao TT, Man RYK. 5-Hydroxytryptamine and thromboxane A2 as physiologic mediators of human umbilical artery closure. *J Soc Gynecol Investig*, 2003;10:490–495.
- Rosado-Mendez IM, Nam K, Hall TJ, Zagzebski JA. Task-oriented comparison of power spectral density estimation methods for quantifying acoustic attenuation in diagnostic ultrasound using a reference phantom method. *Ultrason Imaging*, 2013;35:214–234. [PubMed: 23858055]
- Schild H, Fitzpatrick R, Nixon W. Activity of the human cervix and corpus uteri: their response to drugs in early pregnancy. *Lancet*, 1951;1:250–253. [PubMed: 14795835]
- Schneider Ca, Rasband WS, Eliceiri KW. NIH Image to ImageJ: 25 years of image analysis. *Nature Methods*, 2012;9:671–675. [PubMed: 22930834]
- Thijssen JM. Ultrasonic speckle formation, analysis and processing applied to tissue characterization. *Pattern Recogni Lett*, 2003;24:659–675.
- Thomson DJ. Spectrum estimation and harmonic analysis. *Proceedings of the IEEE*, 1982;70:1055–1096.
- Vink J, Feltovich H. Cervical etiology of spontaneous preterm birth. *Semin Fetal Neonatal Med*, 2016;21:106–112. [PubMed: 26776146]
- Vink JY, Qin S, Brock CO, Zork NM, Feltovich HM, Chen X, Urie P, Myers KM, Hall TJ, Wapner R, Kitajewski JK, Shawber CJ, Gallos G. A new paradigm for the role of smooth muscle cells in the human cervix. *Am J Obstet Gyencol*, 2016;215:1–478.
- Wear KA, Milunski MR, Wickline SA, Perez JE, Sobel BE, Miller JG. Contraction-related variation in frequency dependence of acoustic properties of canine myocardium. *J Acoust Soc Am*, 1989;86:2067–2072. [PubMed: 2689494]
- Wickline SA, Thomas LJ, Miller JG, Sobel BE, Perez JE. A relationship between ultrasonic integrated backscatter and myocardial contractile function. *J Clin Invest*, 1985;76:2151–2160. [PubMed: 3908482]
- Yao LX, Zagzebski JA, Madsen EL. Backscatter coefficient measurements using a reference phantom to extract depth-dependent instrumentation factors. *Ultrason Imaging*, 1990;12:58–70. [PubMed: 2184569]
- Youssef AF. The uterine isthmus and its sphincter mechanism, a radiographic study: I. The uterine isthmus under normal conditions. *Am J Obstet Gynecol*, 1958;75:1305–1319. [PubMed: 13545265]
- Zagzebski JA, Rosado-Mendez IM, Nasief HG, Hall TJ. Quantitative ultra-sound: Enhancing diagnosis using estimates of acoustic attenuation and backscatter. *AIP Conference Proceedings*, 2016;1747:50001.
- Ziliani M, Azuaga A, Calderon F, Pages G, Mendoza G. Monitoring the effacement of the uterine cervix by transperineal sonography: a new perspective. *Journal of ultrasound in medicine*, 1995;14:719–724. [PubMed: 8544236]



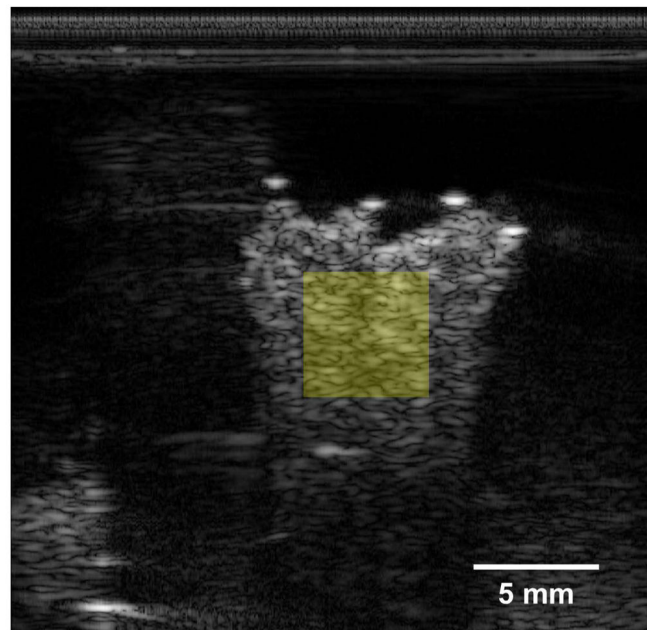
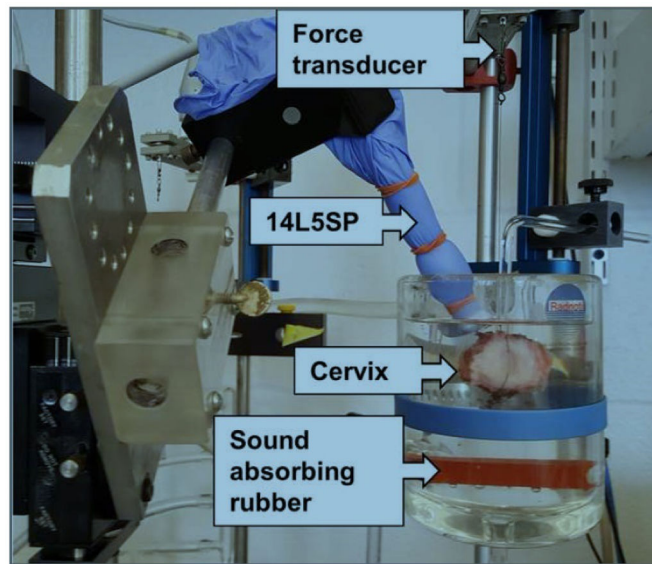


**Figure 1:**

(a) A representative photograph of the experimental setup for measuring muscle force generation and RF data acquisition. The cervix specimen, the 14L5SP ultrasound transducer, and the force transducer are labeled with arrows. Two sutures are shown that are inserted through the endocervical canal. One of those sutures attaches the cervix to the bottom of the organ bath. The other suture extends up to the force transducer. Orange inserts in the organ bath are sound absorbing rubber, helping to minimize clutter in the (b) B-mode image. The semitransparent, yellow square represents where in the sample backscatter parameters are estimated.

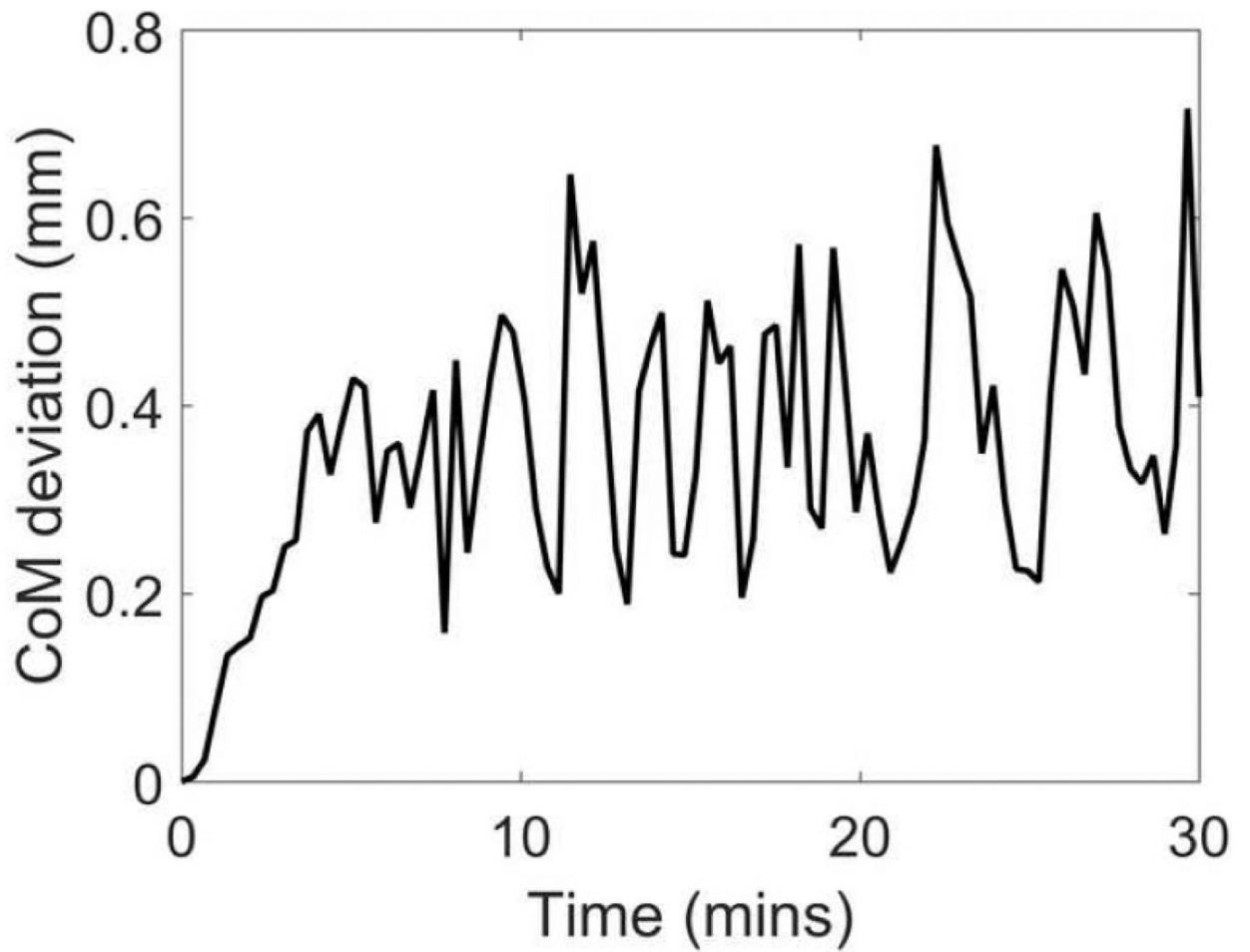


**Figure 2:**  
A center of mass (CoM) deviation curve for specimen number 3. These estimates were obtained from the B-mode images. Time = 0 represents when oxytocin was delivered to the sample.

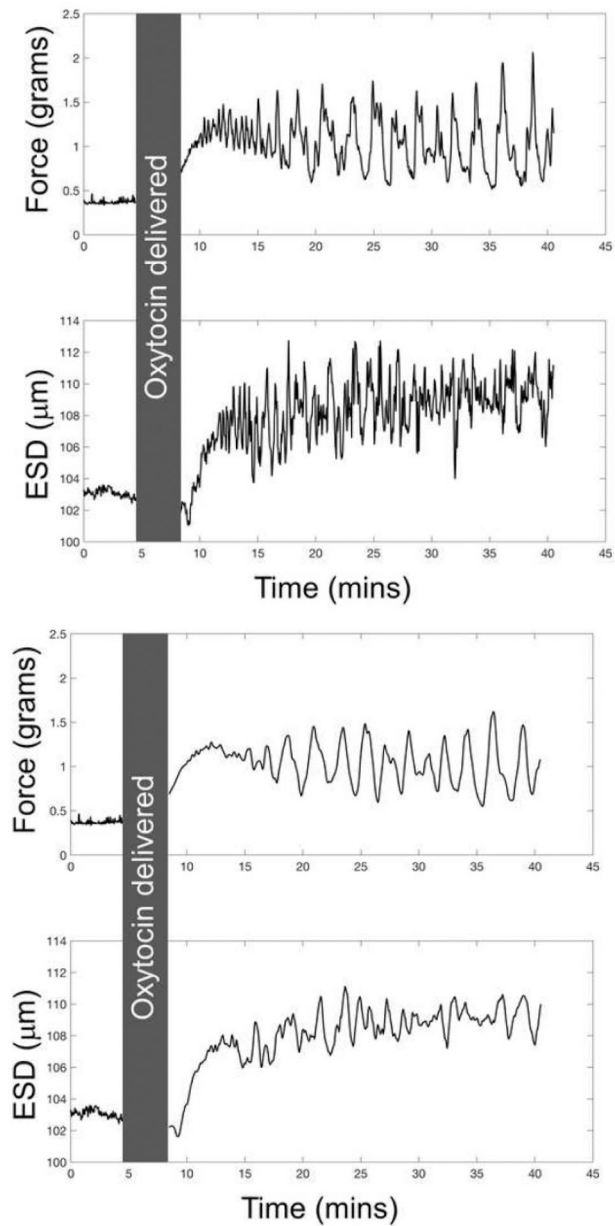


**Figure 3:** Parameter time series for force generation and ESD for specimen number 3 for (a) unfiltered and (b) filtered data. The gray box represents the time over which oxytocin was added to the organ bath (and ultrasound data was not acquired).

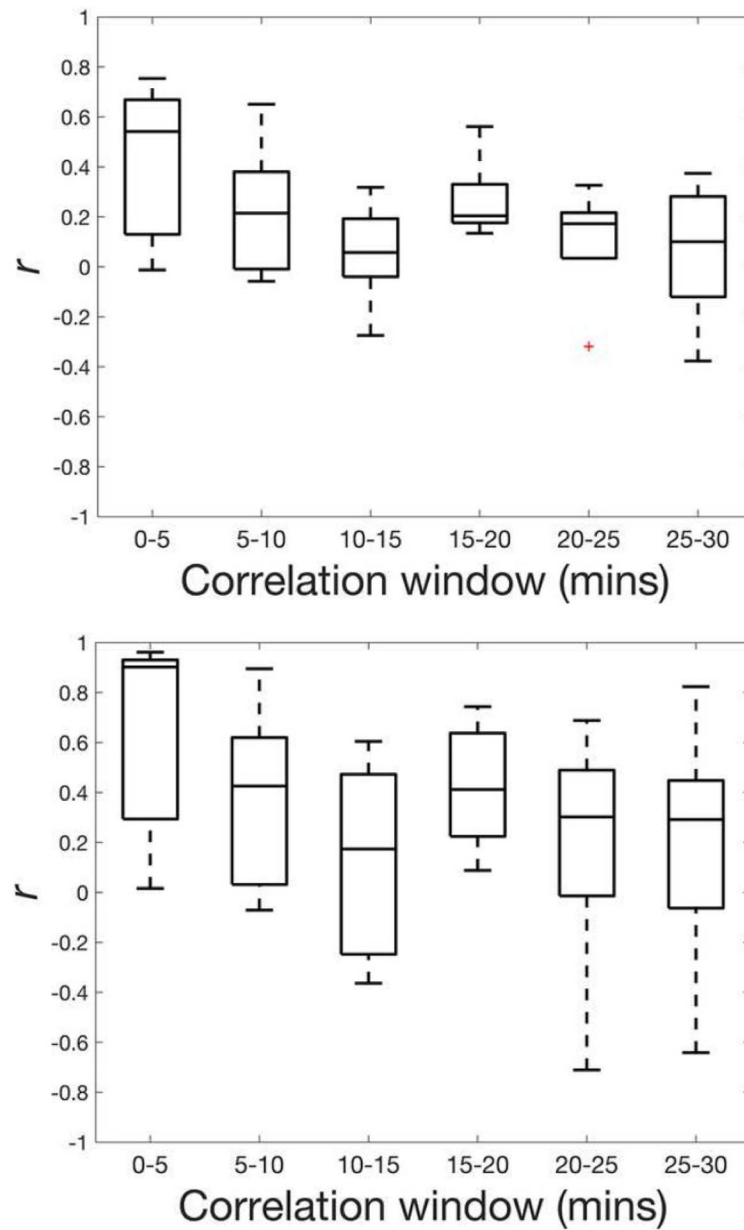


**Figure 4:** Box plots of Pearson  $r$  between unfiltered force and unfiltered ESD data (a) and between filtered force and filtered ESD data (b) over six-time windows for the five specimens. Bars represent maxima and minima within  $1.5 \times \text{IQR}$ .